

pubs.acs.org/acschemicalbiology Articles

Cationic Polymers Enable Internalization of Negatively Charged Chemical Probes into Bacteria

Hannah K. Lembke,[△] Adeline Espinasse,[△] Mckenna G. Hanson, Christian J. Grimme, Zhe Tan, Theresa M. Reineke, and Erin E. Carlson*

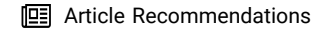


Cite This: ACS Chem. Biol. 2023, 18, 2063-2072

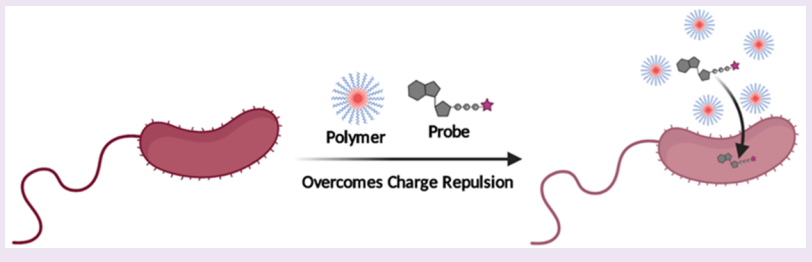


ACCESS I

III Metrics & More



SI Supporting Information



ABSTRACT: The bacterial cell envelope provides a protective barrier that is challenging for small molecules and biomolecules to cross. Given the anionic nature of both Gram-positive and Gram-negative bacterial cell envelopes, negatively charged molecules are particularly difficult to deliver into these organisms. Many strategies have been employed to penetrate bacteria, ranging from reagents such as cell-penetrating peptides, enzymes, and metal-chelating compounds to physical perturbations. While cationic polymers are known antimicrobial agents, polymers that promote the permeabilization of bacterial cells without causing high levels of toxicity and cell lysis have not yet been described. Here, we investigate four polymers that display a cationic poly(2-(dimethylamino)ethyl methacrylate (D) block for the internalization of an anionic adenosine triphosphate (ATP)-based chemical probe into Escherichia coli and Bacillus subtilis. We evaluated two polymer architectures, linear and micellar, to determine how shape and hydrophobicity affect internalization efficiency. We found that, in addition to these reagents successfully promoting probe internalization, the probelabeled cells were able to continue to grow and divide. The micellar structures in particular were highly effective for the delivery of the negatively charged chemical probe. Finally, we demonstrated that these cationic polymers could act as general permeabilization reagents, promoting the entry of other molecules, such as antibiotics.

■ INTRODUCTION

The bacterial cell envelope is a protective barrier from the environment and is therefore critical for survival. Bacteria have evolved highly effective methods that selectively enable desired compounds to cross their cell envelopes while simultaneously preventing the internalization of others. These structures not only pose major challenges in the development of antibacterial agents but also hinder our ability to efficiently deliver other cargo, such as chemical probes, to the cytosol. Probe delivery requires effective methods that facilitate cell penetration without causing substantial microbial death. Such strategies are crucial for the continued study of bacterial physiology,²⁻⁷ as envelope damage leads to decreased cytoplasmic osmolarity,8 membrane protein damage,9 leakage of cytosolic or periplasmic components, 10 and ultimately lysis.^{1,8} These imbalances alter the biochemistry of the cell, making the resulting data less representative of the basal biological system.

The two major classes of bacteria, Gram-positive and Gramnegative, differ based on the structure of their cell envelope. In Gram-positive bacteria, the cell envelope is composed of a cytoplasmic membrane that is made of phospholipids encompassed by a thick layer of peptidoglycan-containing teichoic acids. The Gram-negative envelope also contains a phospholipid inner membrane (IM), but it is in combination with a thin peptidoglycan layer that is surrounded by an additional outer membrane (OM) coated in lipopolysaccharides (LPSs) and surface proteins. Previous work has demonstrated the transport of compounds to the cytosol in both types of bacteria through a variety of methods, including synthetic transporters, hyperporination, efflux pump inhibitors, hypersusceptible mutant strains (such as *Escherichia coli* DC2), hypersusceptible mutant strains (such as *Escherichia coli* DC2), and membrane permeabilization agents. Of particular importance to these studies, there is significant literature focused on reagents that permeabilize the

Received: June 14, 2023 Accepted: August 21, 2023 Published: September 6, 2023





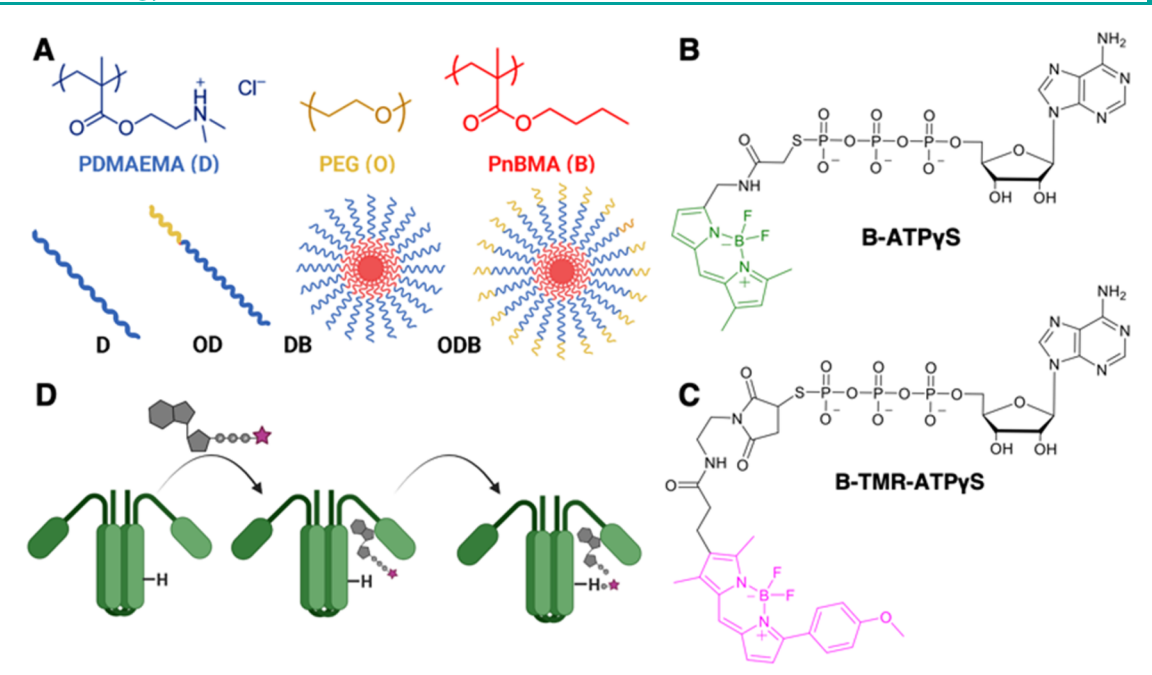


Figure 1. Probe and polymer structures. (A) Component blocks for the polymers and cartoon depictions of their overall architecture. (B) The structure of the activity-based probe **B-ATPγS**. (C) The structure of activity-based probe **B-TMR-ATPγS**. (D) A cartoon depiction of the fluorophore transfer of an adenosine triphosphate (ATP)-based probe to a model histidine kinase (HK), HK853.

cell envelope, including polyamines, 19,20 the cationic chelator ethylenediaminetetraacetic acid (EDTA),²⁴ and cationic peptides, ^{2,6,21,22} of which polymyxins are of crucial importance. ^{23,25} Polymyxins are highly toxic, but analogues that act exclusively to permeabilize the cell envelope without antibacterial activity have also been discovered. 25-27 For instance, a commercially available polymyxin derivative, polymyxin B nonapeptide (PMBN), is considerably less toxic than its parent compound while still retaining its permeabilization ability. 17,18 This property makes it an effective reagent for sensitizing Gram-negative bacteria to antibiotics that are otherwise unable to penetrate the cell. PMBN disrupts the OM of Gram-negative bacteria by interacting with negatively charged LPSs, but it has a limited effect on bacterial viability. Polymyxins have little to no activity against Gram-positive bacteria, given their lack of LPSs. 17,28,29 The use of cationic polymers as antimicrobial agents is well-established due to their cheap cost and easy-to-modulate chemistry. 30,31 However, the identification of analogues that promote penetration without causing cell death is a much less developed field.

The delivery of negatively charged molecules into both prokaryotic and eukaryotic cells is a particular challenge given the charge-charge repulsion that exists between these species and the cell membrane/envelope structures.³² Of particular note, nucleoside triphosphates (NTPs), such as adenosine triphosphate (ATP), are poorly internalized.^{33–35} Romesberg and co-workers reported an engineered strain of E. coli that expresses an NTP transporter, facilitating the internalization of non-natural NTPs.³⁶ While successful, the importers have a limited recognition scope, and this strategy cannot be used in wild-type organisms. Kraus and co-workers reported the use of a positively charged cyclodextrin derivative, termed synthetic nucleotide triphosphate transporter (SNTT), to internalize NTPs into eukaryotes and prokaryotes. 12' SNTT binds specifically to the triphosphate moiety, masking its charge. It is suspected that the polyarginine tail inserts itself into the cellular envelope to deliver the cargo, followed by NTP

displacement with endogenous phosphates. This method was demonstrated by the successful delivery of the nucleosidefunctionalized NTP, cyanine-3-deoxyuridine triphosphate, into E. coli and Mycobacterium smegmatis. 12 A prodrug approach has also been used, in which negative charges are masked by protecting groups that are cleaved off by endogenous enzymes upon molecule internalization.^{37–40} However, the synthesis of molecules that contain masked phosphates remains challenging, and incomplete enzymatic cleavage of the prodrug can result in a low intracellular concentration of the active species. Relatedly, in an approach termed ProTide, a monophosphate (or a monophosphonate) is converted to its active di- and triphosphate form once in the cytosol.³⁹ This strategy can also be synthetically challenging and suffer from incomplete in vivo conversion to the active compound while also precluding the use of nucleotides that are functionalized off of the phosphates.

With the goal of devising a highly generalizable internalization method that is applicable to any type of bacteria, we sought inspiration from the rapidly expanding pool of reagents developed for delivery of genetic material across the cell membrane in eukaryotic cells. 41 Polymer-based delivery systems have been used to transfect mammalian cells with plasmid DNA (pDNA), RNA, and antisense oligonucleotides (ASOs) through the formation of polyplexes that are held together with electrostatic interactions. 42,43 In these systems, the genetic material is condensed, protected within the polymer structure, and typically internalized via an endosome-mediated mechanism. After escaping the endosome, it is then translocated to the cytosol and nucleus.⁴⁴ Many of the effective polymers present nitrogen-containing motifs that are positively charged at a physiological pH value, promoting "polyplex" formation with the negatively charged phosphate groups of the genetic material. We have extensively studied cationic polymer-based systems for the delivery of payloads into mammalian cells, particularly focusing on the effects of the polymer architecture. Our work has determined that complex architectures such as micelles (termed micelleplex when

complexed with genetic material) are ideal for material delivery. $^{45-49}$

The cationic nature of these materials suggests that they may also interact favorably with bacterial cells. 2,22,30,50,51 In addition, the ease of synthesis of these types of molecules could make them a promising new class of bacterial delivery reagents. While eukaryotic membranes and prokaryotic cell envelopes differ, the ability of these polymers to complex with negatively charged genetic materials makes them promising candidates for the delivery of other negatively charged molecules, such as an ATP-based probe, BODIPY-FL-ATP γ S.⁵² We previously reported the use of this molecule to study the activity of bacterial histidine kinases (HKs), which are important sensory proteins involved in signaling that use ATP as their native substrate. Upon interaction with an HK, BODIPY-FL-ATPγS acts as an activity-based probe and results in the covalent labeling of the protein with a fluorescent tag. As such, this molecule provides the ideal test case for the internalization of anionic species, as we can rapidly detect the labeling of its cytosolic protein target using a gel-based assay. Herein, we investigate the ability of four polymer architectures to promote the internalization of BODIPY-FL-ATPγS into bacteria. We identified polymers that promote probe internalization into Gram-positive and Gram-negative bacteria without causing substantial cell damage or death.

RESULTS AND DISCUSSION

Polymer Selection. We sought to investigate polymers that have shown promise for the delivery of challenging payloads (i.e., pDNA and ASOs^{45,47}) into mammalian cells, including two linear polymers and two polymers that can selfassemble into micelles. 45-47,53-55 Hydrophilic poly(ethylene glycol) (PEG or O), cationic poly(2-(dimethylamino)ethyl methacrylate (PDMAEMA or D), and hydrophobic poly(nbutyl methacrylate) (PnBMA or B) cores were utilized as building blocks to prepare polymeric micelles or linear polymers (Figure 1A). The amine-containing D block is cationic under physiological conditions due to its pK_a value of ~8.5,45 which, in eukaryotic cell applications, promotes interactions with polyanions such as nucleic acids and phospholipids. 45-47 Additionally, this cationic block promotes superior internalization of genetic material into mammalian cells compared to many other architectures. 47,49,54 The hydrophobic B block enables micelle formation by selfassembly, acting as its core and exposing the other blocks (O or OD) to the environment. The micelles were formed using the PDMAEMA-b-PnBMA (DB) amphiphilic diblock copolymer or the PEG-b-PDMAEMA-b-PnBMA (ODB) triblock copolymer, yielding structures with hydrodynamic radii of 28 and 34 nm, respectively. The linear polymers were built with only hydrophilic building blocks, either with the PEG-b-PDMAEMA (OD) diblock polymer or the PDMAEMA (**D**) homopolymer.

Our prior work demonstrated that all four vehicles, the linear polymers **D** and **OD** and the micelles **DB** and **ODB**, successfully complex with pDNA⁴⁷ and ASOs⁴⁵ and deliver these biomolecules into eukaryotic cells. Interestingly, there were substantial differences in the delivery efficacy based on the polymer architecture, with the micelles performing significantly better than the linear polymers. It is hypothesized that the higher concentrations of amines that are condensed and packed together within the micelle may stimulate internalization through increased interactions with the

negatively charged plasma membrane in mammalian cells. Indeed, this system was able to deliver challenging payloads to mammalian cells, such as CRISPR-Cas9 cargo and pDNA, even outperforming industry standards. We hypothesized that the negatively charged phosphate tail of an ATP derivative, such as BODIPY-FL-ATP γ S, could interact with these cationic polymers and promote internalization into bacteria.

Chemical Probe Design. To enable rapid assessment of the internalization and subsequent cytoplasmic accessibility of an ATP derivative, we sought to use a fluorescent analogue, BODIPY-FL-ATPγS (B-ATPγS; Figure 1B). This molecule labels catalytically active bacterial HKs, resulting in the transfer of a fluorescent phosphate moiety directly to the targeted proteins; this promotes rapid visualization in gel-based assays (Figure 1D). 52,56 The initial internalization studies that were conducted in E. coli with B-ATPyS suffered from high background fluorescence that overlapped with the BODIPY-FL spectra, likely due to intrinsically fluorescent flavoproteins^{57,58} (Figure S1). To overcome this challenge, we synthesized a related analogue with a red-shifted fluorophore, BODIPY-TAMRA ($\lambda_{\rm ex}/\lambda_{\rm em}$ = 542 nm/568 nm), in one step via a Michael-type reaction from ATPγS with BODIPY-TAMRA-maleimide (B-TMR-ATPγS; Figure 1C, Scheme S1). B-TMR-ATPγS was verified as an ABP by labeling of a purified HK, HK853, originating from Thermotoga maritima^{52,58} (Figure S2). For ease of use, we employed a truncated version of HK853 that lacked the transmembrane and signaling

Probe Internalization into *E. coli***.** To evaluate the ability of our polymers to facilitate the entry of B-TMR-ATPyS through the cell envelope, we investigated the internalization into a strain of E. coli (BL21) that harbors an inducible vector for overexpression of HK853 (a constitutively active construct). We used our previously established gel-based assay^{52,56} to determine when B-TMR-ATPγS reached the cytoplasm, thus resulting in HK labeling. Our first objective was to optimize the reagent concentrations, and we tested a range of nitrogen/phosphorus (N/P; from the polymer D block and the probe, respectively) molar formulation ratios. At each N/P ratio, B-TMR-ATP γ S (33 μ M) was first incubated with the polymer to promote complexation (30 min). This mixture was then added to HK853-expressing *E. coli* (30 min). Following cell lysis, the proteome was separated via SDS-PAGE and the labeled proteins were visualized by fluorescence scanning. A 5/1 N/P ratio yielded optimal protein labeling with the smallest possible amount of polymer (Figure S3).4 We determined that comparable protein labeling could be achieved with a lower probe concentration (20 μ M) when the 5/1 N/P ratio was maintained (Figure S4).

Using these optimized conditions, we compared the efficacy of our small polymer library, as well as two known internalization agents, PMBN and SNTT (Table S1 and Figure S5). The micelle polymers yielded the highest HK853 labeling (assigned as 100%), followed by the linear polymers [94% (OD) and 72% (D) relative to the micelle polymers]. The commercially available reagents SNTT and PMBN trailed at 22% and 37% relative HK853 labeling, respectively. We also found that a control polymer containing only the O block (i.e., PEG functionality without amines) was insufficient for protein labeling (Figure S6). The B block alone is insoluble in media. Finally, we confirmed that the fluorophore alone did not

ACS Chemical Biology pubs.acs.org/acschemicalbiology Articles

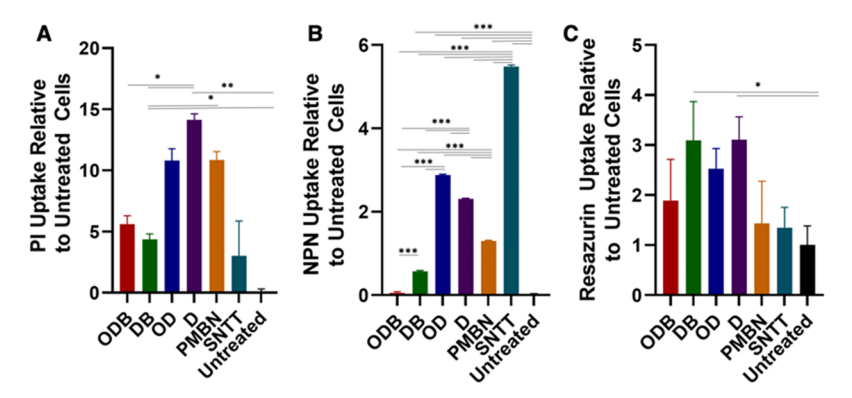


Figure 2. Cell damage following polymer treatment. (A) Cell envelope permeabilization. Propidium iodide (PI) uptake following 30 min treatment. (B) Outer membrane permeabilization. 1-N-Phenylnaphthylamine (NPN) uptake following 15 min treatment. (C) Metabolic activity. Resazurin reduction following 10 min treatment. Experiments were performed with a 5/1 N/P ratio, calculated from 20 μM B-TMR ATPγS, 200 μM polymyxin B nonapeptide (PMBN), and 40 μM synthetic nucleotide triphosphate transporter (SNTT) and compared to untreated cells. Error bars represent standard deviations from two biological replicates. Uptake calculations can be found in the Experimental Section. The NPN and resazurin assays utilize statistical analysis that was performed in GraphPad Prism, specifically an ordinary one-way ANOVA using Tukey's multiple corrections test post hoc. The PI assay analysis was performed with a Welch and Brown-Forsythe one-way ANOVA using Tukey's multiple corrections test post hoc (*p < 0.05, **p < 0.005, and ***p < 0.001).

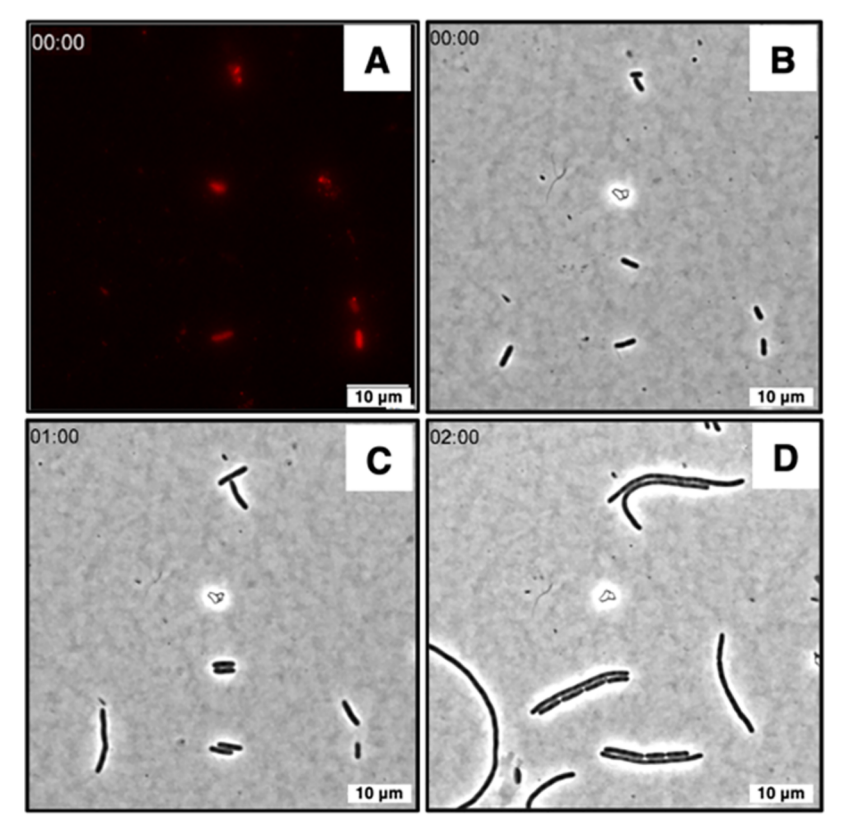


Figure 3. Time-lapse imaging of *E. coli* treated with DB and B-TMR-ATPγS. (A) The zero time point (t=0) demonstrates labeling with a cotreatment of B-TMR-ATPγS (20 μ M with 0.073 mg mL⁻¹ DB polymer in a TES buffer; imaged in the TRITC channel; $\lambda_{\rm ex}/\lambda_{\rm em}=542$ nm/568 nm). The fluorescence photobleached during the course of the experiment, making fluorescent imaging impossible at later time points. (B) The bright field (BF) channel at t=0. (C) The BF channel at t=1 h. (D) The BF channel at t=2 h. Scale bars are 10 μ m. Representative images were taken from a single time-lapse experiment out of three biological replicates. The time-lapse movie is shown in Movie S1.

promote protein labeling ^{59,60} (treatment with **ODB** or **DB** and the BODIPY fluorophore; Figure S7).

Bacterial Damage and Viability. Permeabilization reagents are bactericidal if they cause too much damage.²⁶ We sought to determine if HK853 labeling was due to the internalization of the probe or the result of widespread cellular damage that exposed HK853 and other cytoplasmic proteins to

B-TMR-ATPγS. First, we used propidium iodide (PI), a membrane-impermeable DNA dye, to differentiate between the live and dead cells. The micellular structures and SNTT caused less damage to the *E. coli* envelope than the linear polymers or PMBN (Figure 2A; colistin was used as a positive control). Next, we assessed OM damage using 1-N-phenylnaphthylamine (NPN), which becomes fluorescent in

ACS Chemical Biology pubs.acs.org/acschemicalbiology Articles

hydrophobic environments.⁷ We hypothesized that there may be interactions between the positively charged **D** block in the polymers and the negatively charged LPS, thus resulting in the formation of pores.⁶³ It was determined that the linear polymers and PMBN cause a similar amount of damage, whereas the micelle polymers yield substantially less damage, with **ODB** behaving similarly to the untreated control (Figure 2B). SNTT treatment resulted in the greatest OM perturbation. These data may indicate differences in the membrane disruption mechanisms of the investigated reagents. For example, the polyarginine tail of SNTT is thought to leaf through the OM, whereas PMBN likely displaces the divalent cations found in the OM.^{12,17,28} Future studies will be needed to obtain detailed information about how our polymers interact with the bacterial envelope.

Next, we evaluated how the polymers affect metabolic activity as a measure of cell viability using resazurin, which is reduced inside of live cells and yields a fluorescent species. All treatments except for that with SNTT had a higher signal than the untreated control (Figure 2C). This increased fluorescence is likely due to the enhanced permeability of the cellular envelope, which enables more resazurin to enter the treated cells (the polymers are not intrinsically fluorescent, Figure S8). This is supported by our observation that colistin and PMBN also cause an increased fluorescent signal (Figure S9). In summary, these data indicate that the micelle DB polymer shows the best combination of probe internalization/protein labeling and cell integrity.

We then used time-lapse microscopy to further investigate the health of the individual labeled cells and to eliminate the possibility that the labeled cells die while the unlabeled cells are the ones that appear to be viable following treatment. We focused on the micelle DB polymer, which showed the most promise in the previous assays, and the related linear \boldsymbol{D} polymer. We found that cells with the internalized probe, as judged by their fluorescent signal, could grow and propagate (Figures 3 and S10). We also observed that a proportion of the labeled cells were lysed or became filamented, a known response to cell membrane damage.⁶⁷ This phenomenon was much more pronounced following treatment with D than with DB, which is consistent with the results of our membrane damage assays. As expected, treatment with only B-TMR-ATPγS yielded no fluorescent cells and normal cell growth (Figure S11), while treatment with DB or D alone caused some filamentation (Figures S12 and S13). Filamentation was also seen in the cells treated with PMBN, which suggests that many permeabilization agents may induce this phenotype (Figures S14 and S15). Many of the cells treated with SNTT were lysed (Figures S16 and S17).

Lastly, we performed a colony forming unit (CFU) assay to quantify the toxicity of the polymers. Cells were treated with each polymer and then plated onto LB agar, which contained ampicillin (required for the maintenance of the HK-expression plasmid). Importantly, we found no statistically significant differences in CFU mL⁻¹ between the polymer-treated samples and the untreated control (Figure S18), which confirms that, while the probe is sufficiently internalized due to the observed envelope damage caused by these reagents, the polymers do not cause substantial cell death.

B-TMR-ATP\gammaS and Polymer Complexation. While the polymers enabled **B-TMR-ATP\gammaS** to effectively penetrate the *E. coli* envelope, it was unclear if they complexed with **B-TMR-ATP\gammaS** to facilitate entry or served exclusively as permeabiliza-

tion agents. While prior work has demonstrated clear interactions between this suite of polymers and pDNA and ASOs, 45,47 complexation with a substantially smaller molecule has not yet been investigated. First, we compared the level of HK853 labeling when the polymers were used to pretreat the cells to when the polymers were added at the same time as B-TMR-ATPyS. We reasoned that, if probe internalization only required permeabilization by the polymers and not complexation between the polymer and B-TMR-ATP\(\gamma\)S, we should still see substantial protein labeling when the cells are pretreated with the polymers. A gel-based assessment revealed decreased band intensities in the pretreatment samples (the polymer was washed away following incubation; Table S2). Coomassie staining was performed to evaluate the protein loading and confirmed that the decreased fluorescence signal was not due to a lower abundance of protein (Figure S19). While the labeling intensity was diminished, the same protein banding pattern was observed, suggesting that complexation (polymer and probe preincubation) is not required for probe entry into the cytosol (Figure 4). Entry into the cytosol without polymer

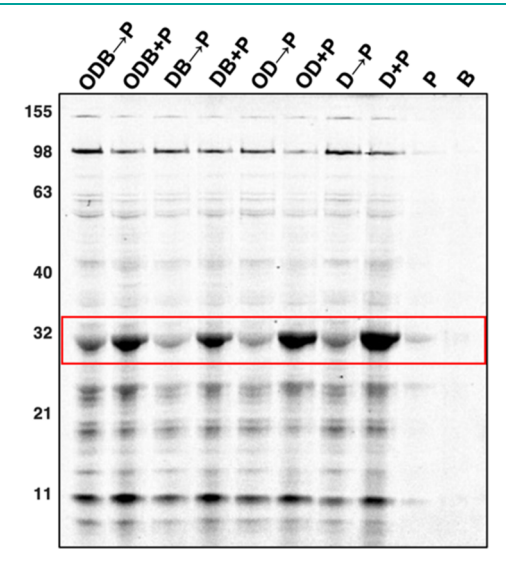


Figure 4. Polymer pretreatment versus co-treatment in *E. coli*. Arrows (\rightarrow) indicate pretreatment (30 min) with the polymer (5/1 N/P) prior to incubation with **B-TMR-ATPγS** (P, 20 μ M, 30 min). Plus signs (+) indicate co-treatment (30 min). P is **B-TMR-ATPγS** alone, and B is the buffer alone. The pretreatment samples were washed once with 100 μ L of TES buffer between incubations. Representative gels were from two biological replicates. The red box indicates HK853. The molecular weight ladder is in kDa.

complexation has also been demonstrated in eukaryotic cells for the delivery of pDNA.⁶⁸ Pretreatment and co-treatment with PMBN and SNTT yielded no appreciable difference in the labeling intensity (Figure S20).

To further evaluate whether binding interactions occur between our anionic probe and the cationic polymers, we employed dynamic light scattering (DLS) studies and electrophoretic mobility shift assays, which are routinely used to study polymer/nucleic acid complexes. While most investigations focus on large oligonucleotides, interactions have been observed with ASOs (~20 negative charges). We performed DLS studies similar to those reported with ODB, DB, OD, and D and pDNA and observed no significant size changes upon incubation with B-TMR-ATPγS (Figure S21 and Table S3). The electrophoretic mobility shift assay

ACS Chemical Biology pubs.acs.org/acschemicalbiology Articles

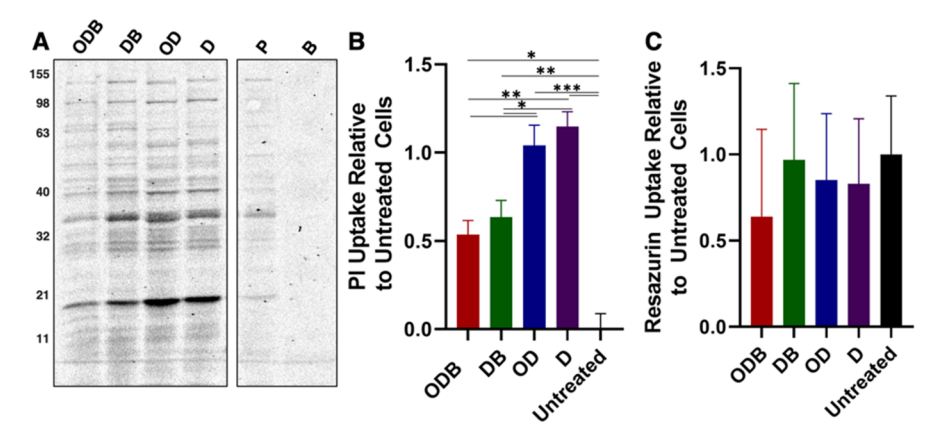


Figure 5. B. subtilis labeling and viability with polymer treatment. (A) Labeling profile of B. subtilis co-treated with each polymer and B-TMR-ATPγS. All of the experiments were performed with a 5/1 N/P ratio and 20 μ M B-TMR-ATPγS for 30 min. The probe-only (P, 20 μ M) and TES buffer-only (B) samples are the controls. Representative gels were from three biological replicates. The molecular weight ladder is in kDa. The Coomassie-stained gel is shown in Figure S26. (B) Envelope permeabilization. The propidium iodide (PI) uptake after polymer treatment. Error bars represent standard deviations from two biological replicates. (C) The metabolic activity. Resazurin uptake following polymer treatment. Error bars represent standard deviations from two biological replicates. Statistical analysis was performed in GraphPad Prism using an ordinary one-way ANOVA with Tukey's multiple corrections test post hoc (*p < 0.05, **p < 0.005, ***p < 0.001).

also showed no differences (Figure S22). However, the small size of our probe may make detection of changes in these assays challenging. As such, we employed a more sensitive technique, ³¹P NMR. As a proxy for the supply-limited **B-TMR ATPγS** probe, ATP was used, as it should have similar electrostatic interactions with the cationic polymers. We observed no differences between the spectra obtained with ATP and those obtained with the **D** polymer (Figures S23 and S24). Thus, we conclude that probe/polymer complexation is not occurring, nor is it required, for cellular entry.

Generality of Internalization. We postulated that the cationic polymers could promote the internalization of other molecules, given the apparent lack of discrete interactions between the polymer and its "payload". Thus, we explored the scope of molecules that could be internalized by assessing a small subset of antibiotics: tetracycline, colistin, and vancomycin. The antibiotics were used at sub-MIC levels, and cell death was compared between co-treatment with polymers **D** and **DB**, PMBN, and the antibiotic alone. These antibiotics were selected for their varying modes of action, structures, and charge states at neutral pH. In addition, vancomycin is typically inactive against Gram-negative organisms such as *E. coli*, as it cannot pass the OM to bind its peptidoglycan target.

For tetracycline, which must reach the cytoplasm in order to be active, we noted that D, DB, and PMBN all appear to promote additional cell killing in comparison to tetracycline alone, but the difference is not statistically significant (Figure S25). This perhaps indicates that tetracycline is already internalized well and that additional cell penetration provides little advantage. Conversely, we observed notable differences from the other antibiotics. Colistin, which disrupts the inner and outer membranes, was made more effective in the presence of both our polymers and PMBN, with polymer D yielding a statistically significant difference in CFU compared to colistin alone. These data further substantiate the disruption of the cell envelope. Finally, co-treatment with our polymers enabled vancomycin to reach the periplasmic space and kill the cells, confirming the disruption of the outer membrane. Together, these results demonstrate this class of cationic polymers as

novel permeabilization agents that can be used in a broad range of applications in bacteria.

Permeabilization of Gram-Positive Bacillus subtilis. While it is generally accepted that Gram-positive organisms are easier to penetrate than their Gram-negative relatives, they present unique challenges, as their cell envelope has a distinct architecture, including a thick cell wall and teichoic acids. 1,32,71 We further explored the generality of our polymers by applying them to the model Gram-positive organism B. subtilis. As before, co-treatment with each polymer and B-TMR-ATPyS, maintained at a 5/1 N/P ratio for consistency, resulted in substantial protein labeling (Figure 5A; see also the Coomassie stain of the gel in Figure \$26). We also evaluated cell damage and viability using a subset of the previous assays. PI uptake remained near 0.5 in B. subtilis following treatment with ODB and DB but nearly doubled in value following treatment with OD and D, indicating that the micelle polymers cause less envelope damage (Figure 5B). The resazurin assay revealed that cell viability was similar for all polymers compared to that of the control (Figure 5C). As in E. coli, polymers ODB, DB, and OD did not kill the cells, as measured by CFU. Polymer D resulted in a significant decrease in cell number compared to the untreated control (Figure S27). Overall, the differences in the cellular damage caused by the four polymers were less pronounced than in E. coli.

SUMMARY AND CONCLUSIONS

The cationic polymers studied herein showed efficacy in permeabilizing the envelope of both Gram-negative *E. coli* and Gram-positive *B. subtilis* while also maintaining a high level of cell viability. Our studies show that they enable the labeling of cytosolic proteins with the anionic chemical probe **B-TMR-ATPγS**. Importantly, these polymers yielded superior labeling compared to the commercially available reagents PMBN and SNTT (Table S1 provides labeling values normalized to protein content). Our data also indicate that probe internalization is likely occurring through a different mechanism than when these cationic polymers facilitate pDNA internalization into eukaryotic cells or when SNTT promotes molecule entry into bacteria. Indeed, there is no evidence of stable complex formation with **B-TMR-ATPγS** (e.g., DLS, electrophoretic

mobility shift, or NMR data). We anticipate that our polymers promote entry most similarly to polymyxins, which are thought to have electrostatic interactions with negatively charged phosphate groups of the LPS, followed by the displacement of the native metal cations (Mg^{2+} and Ca^{2+}). Since the polymers evaluated herein contain a positively charged **D** block, we anticipate that they may interact in a similar manner with *E. coli.*²⁷

An assessment of the cellular damage caused by the cationic polymers indicates that the micelle architecture is less destructive than the related linear molecules or the polymyxin PMBN. We hypothesize that the linear polymers may interact with a larger section of the bacterial cell envelope, as it is theoretically possible for them to uncoil on this surface, whereas the micelle polymers can only interact through the portion of the D block that is radially extended. We expect that less overall interaction with the cell envelope may result in the decreased cellular damage that we observed. However, it is not clear how this would also result in superior probe entry and protein labeling (Table S4). Future mechanistic studies will aim to better understand the interactions between the negatively charged probe, the cationic polymers, and the bacterial cell surface.

Finally, our cationic polymers are minimally bactericidal or bacteriostatic, and this work provides one of the first demonstrations of such polymers serving as permeabilization agents without causing substantial bacterial death. To our knowledge, the only related example was reported by de Souza and co-workers, where they used cationic copolymers to promote the transformation of pDNA into a noncompetent $E.\ coli\ DHS\alpha$ strain. This trait, along with the generality of our reagents for permeabilization of both Gram-positive and Gramnegative organisms and their demonstrated ability to promote the internalization of multiple molecules, including an anionic chemical probe, strongly suggests that the cationic polymers investigated herein will be useful in a broad range of studies.

EXPERIMENTAL SECTION

The four polymers used in this study were synthesized and characterized in a previous work by Jiang et al. 53 The B-TMR-ATP γ S synthesis, the complexation studies of the probe and the polymers with DLS and the electrophoretic mobility shift assay, the cell growth assay, and general experimental details are provided in the Supporting Information.

Cell Culture. The overexpression strain of E. coli BL21 containing the pHisI HK853 plasmid was streaked onto LB agar plates that contained 100 μg mL $^{-1}$ ampicillin from a frozen glycerol stock and grown overnight at 37 °C. From these plates, a single colony was inoculated into fresh Lennox Broth (LB) medium containing 100 µg mL⁻¹ ampicillin and grown overnight at 37 °C while being shaken at 220 rpm. A 1/10 dilution of the overnight culture was performed in fresh LB medium containing 100 μ g mL⁻¹ ampicillin and grown until $OD_{600} \sim 0.5-0.6$ (Thermo Fisher Scientific, GENESYS 30 visible spectrophotometer). Cells were induced with 1 mM IPTG for 30 min at 37 $^{\circ}\text{C}$ while being shaken at 220 rpm. The cells were treated in accordance with each assay. Next, B. subtilis 3610 was streaked onto LB agar plates from frozen glycerol stocks and grown overnight at 37 °C. From these plates, a single colony was inoculated into fresh LB medium and grown overnight at 37 °C while being shaken at 220 rpm. A 1/10 dilution of the overnight culture was performed in fresh LB medium and grown until $OD_{600} \sim 0.5$. Cells were treated accordingly, as described for each assay.

General Procedure for the Gel-Based Assays. Prior to addition to the cells, 20 μ M B-TMR-ATPγS was incubated on a rotator in the dark at room temperature with 0.1 mg mL⁻¹ ODB,

0.073 mg mL⁻¹ **DB**, 0.068 mg mL⁻¹ **OD**, 0.05 mg mL⁻¹ **D**, 200 μ M PMBN, or 40 μ M SNTT in 30 mM TES buffer (pH = 7.4) for a total volume of 45 μ L for 30 min. The amount of polymer was calculated based on a 5/1 N/P ratio of the amines in the polymer to the phosphates in the 20 μ M B-TMR-ATP γ S probe. The bacteria were spun down (2000 \times g, 1 min) from the cultures (500 μ L for E. coli, 1 mL for B. subtilis), the supernatant was removed, and each sample was resuspended with the designated probe/polymer solution or probe/ permeabilization reagent solution (40 μ L) and then placed in an incubator/shaker (30 min, 37 °C, 220 rpm) in the dark. The cells were centrifuged (2000 \times g, 1 min), the supernatant was removed, and the cells were washed once with TES buffer (100 μ L). The E. coli cells were resuspended in TES buffer (40 μ L), and a 10% (w/v) aqueous SDS solution (4 μ L) was added. The cells were then lysed on ice by sonication using the Hielscher Ultrasonics vial tweeter UP200St instrument at 90% A, 70% C for 30 s on/30 s off for a total time of 3 min. The B. subtilis cells were resuspended (40 μ L) in a 10 mg mL⁻¹ lysozyme aqueous solution and incubated in an incubator/shaker (37 °C, 220 rpm, 30 min) in the dark. Following this incubation, a 10% (w/v) aqueous SDS solution (4 μ L) was added, and the cells were lysed following the aforementioned conditions. The cell lysates were centrifuged (20 min, 21 000 \times g), and the supernatant (20 μ L) was removed and added to the 4X gel loading buffer (8.6 μ L). The samples (12 μ L) were loaded onto a 10% polyacrylamide gel for SDS-PAGE analysis. All of the experiments were performed in biological duplicate.

PI Assay. All measurements took place in a clear, flat-bottom Corning 96-well plate (catalog no. CLS2585 from MilliporeSigma). Assay conditions were adapted from Boix-Lemonche et al. 2 B. subtilis and E. coli cells were grown as described above, spun down (4000 \times g, 10 min), and resuspended in a 1/2 culture volume of 25 mM glucose in 1X PBS (pH = 7.4) to reach an $OD_{600} \sim 1$. A working stock of PI was made to a concentration of 1 mg mL⁻¹ and diluted to a final concentration of 0.05 mg mL $^{-1}$ into a final well volume of 100 μ L. Stock solutions of all of the other compounds were diluted to final concentrations of 0.1 mg mL⁻¹ ODB, 0.073 mg mL⁻¹ DB, 0.068 mg mL^{-1} OD, 0.05 mg mL^{-1} D, 200 μ M PMBN, 40 μ M SNTT, 10 μ g mL^{-1} colistin, 73,74 and 2 mg mL^{-1} lysozyme. Untreated cells served as a negative control. The cells were added immediately prior to measurement at $\lambda_{\rm ex}/\lambda_{\rm em}$ = 595 nm/617 \pm 20 nm on a Tecan spark plate reader. Measurements were taken after 10 min with orbital shaking (5 ms) being performed immediately prior to the reading. The relative PI uptake was calculated using the below equation, where RFU_{treated} is the measured fluorescence of the permeabilization agenttreated samples, RFU_{untreated} is the measured fluorescence of the untreated cells, and $RFU_{positive}$ is the measured fluorescence of the respective positive control samples (lysozyme or colistin):

$$\label{eq:relative_PI} \text{relative PI uptake} = \frac{\text{RFU}_{\text{treated}} - \text{RFU}_{\text{untreated}}}{\text{RFU}_{\text{positive}} - \text{RFU}_{\text{untreated}}}$$

Outer Membrane Damage Assay. Overnight cultures that were performed with E. coli BL21 pHisI cells were diluted 1/10 in fresh LB medium with 100 μg mL⁻¹ ampicillin and grown to OD₆₀₀ \sim 0.5. The cells were then spun down (4000 \times g, 10 min), the supernatant was removed, and the cell pellets were resuspended in 1/2 culture volume of 5 mM HEPES buffer (pH = 7.2) to $OD_{600} \sim 1.0$. A stock solution of 0.5 mM NPN in acetone was diluted to 40 μM in a clear, flatbottom Corning 96-well plate (catalog no. CLS2585 from MilliporeSigma) with 5 mM HEPES buffer. All other compounds were diluted to their final concentrations of 0.1 mg mL⁻¹ ODB, 0.073 mg mL⁻¹ **DB**, 0.068 mg mL⁻¹ **OD**, 0.05 mg mL⁻¹ **D**, 200 μ M PMBN, 40 μM SNTT, and 0.01 mg mL⁻¹ colistin. The cells were added immediately prior to measurement at $\lambda_{ex}/\lambda_{em}$ = 355 nm/405 \pm 20 nm on a Tecan spark plate reader. Measurements were taken at 10 min intervals with orbital shaking (5 ms) being performed immediately prior to each reading. The relative NPN uptake was calculated 10 min into the measurement using the following equation:

$$\text{relative NPN uptake} = \frac{\text{RFU}_{\text{treated}} - \text{RFU}_{\text{untreated}}}{\text{RFU}_{\text{positive}} - \text{RFU}_{\text{untreated}}}$$

where RFU $_{\rm treated}$ is the measured fluorescence of the treated samples, RFU $_{\rm untreated}$ is the measured fluorescence of the untreated cells, and RFU $_{\rm positive}$ is the measured fluorescence of the bacteria treated with colistin. All measurements were taken in technical triplicate and biological duplicate.

Resazurin Assay. A 1000X working stock of resazurin sodium salt (12.5 mg mL $^{-1})$ in LB medium was filter-sterilized through a 0.22 $\mu\mathrm{M}$ PES filter and then diluted with LB medium to a 12.5 μ g mL⁻¹ working stock solution. This working stock was pipetted into each well to a volume of 190 μ L. The cells were grown as previously mentioned, the aliquots were spun down (2000 \times g, 1 min; 500 μ L of E. coli and 1 mL of B. subtilis), and the supernatant was removed. Each sample was resuspended in the designated solutions of 0.1 mg mL⁻¹ **ODB**, 0.073 mg mL⁻¹ **DB**, 0.068 mg mL⁻¹ **OD**, 0.05 mg mL⁻¹ D, 200 μ M PMBN, 40 μ M SNTT, 10 μ g mL $^{-1}$ colistin, or 2 mg mL $^{-1}$ lysozyme in 30 mM TES buffer (pH = 7.4) to a total volume of 40 μ L and incubated (37 °C, 30 min). The cells were centrifuged (2000 \times g, 1 min), the supernatant was removed, and the cells were washed once with TES buffer (100 μ L). The treated cells were then resuspended in TES buffer (100 μ L), and 10 μ L of this sample was added into each well for a total volume of 200 μ L. The 96-well plate was incubated in the dark (37 °C, 10 min), and all measurements took place in a clear, flat-bottom Corning 96-well plate (catalog no. CLS2585 from MilliporeSigma) with measured fluorescence at $\lambda_{\rm ex}/\lambda_{\rm em}$ = 535 nm/ 580 ± 20 nm on a Tecan spark plate reader. The relative fluorescence intensity was calculated using the following equation:

$$resazurin\ uptake = \frac{RFU_{treated} - RFU_{resazurin}}{RFU_{positive} - RFU_{resazurin}}$$

where RFU $_{\rm treated}$ is the measured fluorescence of the treated samples, RFU $_{\rm resazurin}$ is the measured fluorescence of the resazurin solution alone without any cells, and RFU $_{\rm positive}$ is the measured fluorescence of the cells treated with either colistin or lysozyme. All measurements were done in technical triplicate and biological duplicate.

Live Cell Imaging. E. coli cells were grown as described in the Cell Culture section and treated according to the gel-based assay protocol, stopping before cell lysis. An agarose pad was made with 0.1% low-melting agar in LB medium and then slowly poured into the center of a slide containing an outer rectangular border of doublesided tape. It was set aside to cool at 4 °C for at least 30 min prior to use. After treatment with the polymers, the cells were resuspended in fresh TES buffer (pH = 7.4) and pipetted through a 1 and 1/2 in. 20gauge needle eight times to disperse any clumps. The sample (20 μ L) was transferred to the center of the agarose pad, and the slide was slowly rotated to disperse cells completely across the pad. A coverslip $(24 \times 40 \text{ mm})$ was pressed into the sides of the double-sided tape. Samples were imaged in bright field and the TRITC channel $(\lambda_{ex}/\lambda_{em})$ = 545 nm/576 \pm 25 nm) with a cellVivo environmental chamber maintained at 37 °C and under an ambient atmosphere using an Olympus IX73 microscope and an oil immersion on a UPlanSApo 100x/1.40 Oil Ph3/0.17/FN26.5 objective lens. Micrographs were captured with a Hamamatsu ORCA-Flash 4.0 LT C11440-42U30 CMOS camera. The exposure time was ~92 ms. The growth of the cells was monitored by taking images every 15 min for at least 2 h, approximately 10× one division cycle.

ASSOCIATED CONTENT

Supporting Information

The Supporting Information is available free of charge at https://pubs.acs.org/doi/10.1021/acschembio.3c00351.

¹H NMR and ³¹P NMR spectra for all compounds, supporting figures and tables, and additional experimental details, materials, and methods (PDF) Movie S1: live cell imaging after treatment with **DB** polymer and **B-TMR-ATPγS** (MP4)

Movie S2: live cell imaging after treatment with **DB** polymer only (MP4)

Movie S3: live cell imaging after treatment with **D** polymer and **B-TMR-ATPγS** (MP4)

Movie S4: live cell imaging after treatment with D polymer only (MP4)

Movie S5: live cell imaging after treatment with B-TMR-ATP γ S probe only (MP4)

Movie S6: live cell imaging after treatment with PMBN and B-TMR-ATP γ S (MP4)

Movie S7: live cell imaging after treatment with PMBN only (MP4)

Movie S8: live cell imaging after treatment with SNTT and B-TMR-ATP γ S (MP4)

Movie S9: live cell imaging after treatment with SNTT only (MP4)

AUTHOR INFORMATION

Corresponding Author

Erin E. Carlson — Department of Chemistry, University of Minnesota, Minneapolis, Minnesota 55455, United States; Department of Medicinal Chemistry, Department of Biochemistry, Molecular Biology, and Biophysics, and Department of Pharmacology, University of Minnesota, Minneapolis, Minnesota 55455, United States; orcid.org/0000-0001-8287-8893; Email: carlsone@umn.edu

Authors

Hannah K. Lembke — Department of Chemistry, University of Minnesota, Minneapolis, Minnesota 55455, United States

Adeline Espinasse — Department of Chemistry, University of Minnesota, Minneapolis, Minnesota 55455, United States

Mckenna G. Hanson — Department of Chemistry, University of Minnesota, Minneapolis, Minnesota 55455, United States

Christian J. Grimme — Department of Chemical Engineering and Materials Science, University of Minnesota, Minneapolis, Minnesota 55455, United States

Zhe Tan — Department of Chemistry, University of Minnesota, Minneapolis, Minnesota 55455, United States; orcid.org/0000-0002-3518-0772

Theresa M. Reineke — Department of Chemistry, University of Minnesota, Minneapolis, Minnesota 55455, United States; Department of Chemical Engineering and Materials Science, University of Minnesota, Minneapolis, Minnesota 55455, United States; orcid.org/0000-0001-7020-3450

Complete contact information is available at: https://pubs.acs.org/10.1021/acschembio.3c00351

Author Contributions

△H.K.L. and A.E. are co-first authors of this paper. H.K.L.: generated data for figures within the main manuscript and SI, manuscript writing, and project direction. A.E.: project design and preliminary studies, synthesis of probe and generated data for SI, manuscript writing, and project direction. M.G.H.: design and execution of DLS, and intellectual and writing contributions. C.J.G.: polymer synthesis and intellectual and writing contributions. Z.T.: initial project design and polymer synthesis.

Notes

The authors declare no competing financial interest.

ACKNOWLEDGMENTS

We gratefully acknowledge the following funding: the National Institutes of Health Biotechnology, Training Grant 5T32GM008347 (H.K.L. and A.E.); the University of Minnesota Department of Chemistry Excellence Fellowship (H.K.L.); and the National Science Foundation, CHE 2003208 (E.E.C.). We also thank Genentech for the partial funding of this project. M.G.H. acknowledges the support from the National Science Foundation Graduate Research Fellowship Program (DGE-1839286) and the University of Minnesota Doctoral Dissertation Fellowship. This work was also supported by the National Science Foundation (NSF) through the University of Minnesota MRSEC under Award DMR2011401. Any opinions, findings, and conclusions or recommendations expressed in this material are those of the authors and do not necessarily reflect the views of the National Science Foundation. Lastly, we acknowledge BioRender for help in our figure generation.

REFERENCES

- (1) Silhavy, T. J.; Kahne, D.; Walker, S. The bacterial cell envelope. Cold Spring Harb Perspect Biol. 2010, 2 (5), a000414—a000414.
- (2) Chan, L. W.; Hern, K. E.; Ngambenjawong, C.; Lee, K.; Kwon, E. J.; Hung, D. T.; Bhatia, S. N. Selective Permeabilization of Gram-Negative Bacterial Membranes Using Multivalent Peptide Constructs for Antibiotic Sensitization. *ACS Infect Dis* **2021**, *7* (4), 721–732.
- (3) Ferreira, R. J.; Kasson, P. M. Antibiotic Uptake Across Gram-Negative Outer Membranes: Better Predictions Towards Better Antibiotics. *ACS Infect Dis* **2019**, *5* (12), 2096–2104.
- (4) Krishnamoorthy, G.; Wolloscheck, D.; Weeks, J. W.; Croft, C.; Rybenkov, V. V.; Zgurskaya, H. I. Breaking the Permeability Barrier of Escherichia coli by Controlled Hyperporination of the Outer Membrane. *Antimicrob. Agents Chemother.* **2016**, *60* (12), 7372–7381.
- (5) Kumar, S. S.; Ghosh, A. R. Assessment of bacterial viability: a comprehensive review on recent advances and challenges. *Microbiology (Reading)* **2019**, *165* (6), 593–610.
- (6) Malanovic, N.; Lohner, K. Gram-positive bacterial cell envelopes: The impact on the activity of antimicrobial peptides. *Biochim. Biophys. Acta* **2016**, *1858* (5), 936–46.
- (7) Muheim, C.; Götzke, H.; Eriksson, A. U.; Lindberg, S.; Lauritsen, I.; Nørholm, M. H. H.; Daley, D. O. Increasing the permeability of Escherichia coli using MAC13243. *Sci. Rep* **2017**, 7 (1), 17629.
- (8) Wong, F.; Wilson, S.; Helbig, R.; Hegde, S.; Aftenieva, O.; Zheng, H.; Liu, C.; Pilizota, T.; Garner, E. C.; Amir, A.; Renner, L. D. Understanding Beta-Lactam-Induced Lysis at the Single-Cell Level. *Front Microbiol* **2021**, *12*, No. 712007.
- (9) Delhaye, A.; Collet, J.-F.; Laloux, G. A Fly on the Wall: How Stress Response Systems Can Sense and Respond to Damage to Peptidoglycan. Front Cell Infect Microbiol 2019, 9, 380.
- (10) Wong, F.; Stokes, J. M.; Cervantes, B.; Penkov, S.; Friedrichs, J.; Renner, L. D.; Collins, J. J. Cytoplasmic condensation induced by membrane damage is associated with antibiotic lethality. *Nat. Commun.* **2021**, *12* (1), 2321.
- (11) Levinson, W. Structure of Bacterial Cells. In *Review of Medical Microbiology and Immunology*, 14th ed.; McGraw-Hill Education, New York, 2016.
- (12) Zawada, Z.; Tatar, A.; Mocilac, P.; Budesinsky, M.; Kraus, T. Transport of Nucleoside Triphosphates into Cells by Artificial Molecular Transporters. *Angewandte Chemie (International ed. in English)* **2018**, 57 (31), 9891–9895.
- (13) Copp, J. N.; Pletzer, D.; Brown, A. S.; Van der Heijden, J.; Miton, C. M.; Edgar, R. J.; Rich, M. H.; Little, R. F.; Williams, E. M.; Hancock, R. E. W.; Tokuriki, N.; Ackerley, D. F. Mechanistic Understanding Enables the Rational Design of Salicylanilide Combination Therapies for Gram-Negative Infections. *mBio* **2020**, *11* (5), e02068-20.

- (14) Kocaoglu, O.; Carlson, E. E. Profiling of beta-lactam selectivity for penicillin-binding proteins in Escherichia coli strain DC2. *Antimicrob. Agents Chemother.* **2015**, *59* (5), 2785–90.
- (15) Clark, D. Novel antibiotic hypersensitive mutants of Escherichia coli Genetic mapping and chemical characterization. *FEMS Microbiol Lett.* **1984**, 21, 189–195.
- (16) Young, J. L.; Dean, D. A. Electroporation-mediated gene delivery. *Adv. Genet* **2015**, *89*, 49–88.
- (17) Tsubery, H.; Ofek, I.; Cohen, S.; Fridkin, M. Structure-Function Studies of Polymyxin B Nonapeptide: Implications to Sensitization of Gram-Negative Bacteria. *J. Med. Chem.* **2000**, 43, 3085–3092.
- (18) Viljanen, P. The Effect of Polymyxin B Nonapeptide (PMBN) on Transformation. *Biochem. Biophys. Res. Commun.* **1987**, *143* (3), 923–7.
- (19) Kostopoulou, O. N.; Kouvela, E. C.; Magoulas, G. E.; Garnelis, T.; Panagoulias, I.; Rodi, M.; Papadopoulos, G.; Mouzaki, A.; Dinos, G. P.; Papaioannou, D.; Kalpaxis, D. L. Conjugation with polyamines enhances the antibacterial and anticancer activity of chloramphenicol. *Nucleic Acids Res.* **2014**, *42* (13), 8621–34.
- (20) Igarashi, K.; Kashiwagi, K. Polyamine transport in bacteria and yeast. *Biochem. J.* **1999**, 344 (3), 633–642.
- (21) Zhang, L.; Dhillon, P.; Yan, H.; Farmer, S.; Hancock, R. E. W. Interactions of Bacterial Cationic Peptide Antibiotics with Outer and Cytoplasmic Membranes of Pseudomonas aeruginosa. *Antimicrob. Agents Chemother.* **2000**, *44* (12), 3317–3321.
- (22) Mojsoska, B.; Carretero, G.; Larsen, S.; Mateiu, R. V.; Jenssen, H. Peptoids successfully inhibit the growth of gram negative E. coli causing substantial membrane damage. *Sci. Rep* **2017**, *7*, 42332.
- (23) Gill, E. E.; Franco, O. L.; Hancock, R. É. Antibiotic adjuvants: diverse strategies for controlling drug-resistant pathogens. *Chem. Biol. Drug Des* **2015**, 85 (1), 56–78.
- (24) Yang, N. J.; Hinner, M. J. Getting Across the Cell Membrane: An Overview for Small Molecules, Peptides, and Proteins. *Methods Mol Biol.* **2015**, *1266*, 29–53.
- (25) Trimble, M. J.; Mlynárčik, P.; Kolář, M.; Hancock, R. E.W. Polymyxin: Alternative Mechanisms of Action and Resistance. *Cold Spring Harb Perspect Med.* **2016**, 6 (10), a025288.
- (26) Yu, Z.; Qin, W.; Lin, J.; Fang, S.; Qiu, J. Antibacterial Mechanisms of Polymyxin and Bacterial Resistance. *BioMed. Res. Int.* **2015**, 2015, No. 679109.
- (27) Polymyxin Antibiotics: From Laboratory Bench to Bedside; Li, J., Nation, R. L., Kaye, K. S., Eds.; Springer, 2019; Vol 1145.
- (28) Vaara, M.; Viljanen, P. Binding of Polymyxin B Nonapeptide to Gram-Negative Bacteria. *Antimicrob. Agents Chemother.* **1985**, 27 (4), 548–554.
- (29) Yin, J.; Meng, Q.; Cheng, D.; Fu, J.; Luo, Q.; Liu, Y.; Yu, Z. Mechanisms of bactericidal action and resistance of polymyxins for Gram-positive bacteria. *Appl. Microbiol. Biotechnol.* **2020**, *104* (9), 3771–3780.
- (30) Samal, S. K.; Dash, M.; Van Vlierberghe, S.; Kaplan, D. L.; Chiellini, E.; van Blitterswijk, C.; Moroni, L.; Dubruel, P. Cationic polymers and their therapeutic potential. *Chem. Soc. Rev.* **2012**, *41* (21), 7147–94.
- (31) Yang, Y.; Cai, Z.; Huang, Z.; Tang, X.; Zhang, X. Antimicrobial cationic polymers: from structural design to functional control. *Polym. J.* **2018**, *50* (1), 33–44.
- (32) Auer, G. K.; Weibel, D. B. Bacterial Cell Mechanics. *Biochemistry* **2017**, *56* (29), 3710–3724.
- (33) Deng, Y.; Beahm, D. R.; Ionov, S.; Sarpeshkar, R. Measuring and modeling energy and power consumption in living microbial cells with a synthetic ATP reporter. *BMC Biol.* **2021**, *19* (1), 101.
- (34) Cole, L. A. Adenosine Triphosphate Energetics. *Biology of Life* **2016**, 65–77.
- (35) Jurtshuk, P. J., Jr. Bacterial Metabolism. In *Medical Microbiology*, 4th ed.; Baron, S., Ed.; University of Texas Medical Branch at Galveston, Galveston, Texas, 1996.
- (36) Malyshev, D. A.; Dhami, K.; Lavergne, T.; Chen, T.; Dai, N.; Foster, J. M.; Correa, I. R., Jr.; Romesberg, F. E. A semi-synthetic

- organism with an expanded genetic alphabet. *Nature* **2014**, *509* (7500), 385–8.
- (37) Gollnest, T.; Dinis de Oliveira, T.; Rath, A.; Hauber, I.; Schols, D.; Balzarini, J.; Meier, C. Membrane-permeable Triphosphate Prodrugs of Nucleoside Analogues. *Angewandte Chemie (International ed. in English)* **2016**, *55* (17), 5255–8.
- (38) Gollnest, T.; de Oliveira, T. D.; Schols, D.; Balzarini, J.; Meier, C. Lipophilic prodrugs of nucleoside triphosphates as biochemical probes and potential antivirals. *Nat. Commun.* **2015**, *6*, 8716.
- (39) Mehellou, Y.; Rattan, H. S.; Balzarini, J. The ProTide Prodrug Technology: From the Concept to the Clinic. *J. Med. Chem.* **2018**, *61* (6), 2211–2226.
- (40) Espinasse, A.; Lembke, H. K.; Cao, A. A.; Carlson, E. E. Modified nucleoside triphosphates in bacterial research for in vitro and live-cell applications. *RSC Chem. Biol.* **2020**, *1* (5), 333–351.
- (41) Sung, Y. K.; Kim, S. W. Recent advances in the development of gene delivery systems. *Biomater. Res.* **2019**, 23 (1), 8.
- (42) Nie, X.; Zhang, Z.; Wang, C.-H.; Fan, Y.-S.; Meng, Q.-Y.; You, Y.-Z. Interactions in DNA Condensation: An Important Factor for Improving the Efficacy of Gene Transfection. *Bioconjugate Chem.* **2019**, 30 (2), 284–292.
- (43) Kumar, R.; Santa Chalarca, C. F.; Bockman, M. R.; Bruggen, C. V.; Grimme, C. J.; Dalal, R. J.; Hanson, M. G.; Hexum, J. K.; Reineke, T. M. Polymeric Delivery of Therapeutic Nucleic Acids. *Chem. Rev.* **2021**, *121* (18), 11527–11652.
- (44) Thomas, T. J.; Tajmir-Riahi, H.-A.; Pillai, C. K. S. Biodegradable Polymers for Gene Delivery. *Molecules (Basel, Switzerland)* **2019**, 24 (20), 3744.
- (45) Grimme, C. J.; Hanson, M. G.; Corcoran, L. G.; Reineke, T. M. Polycation Architecture Affects Complexation and Delivery of Short Antisense Oligonucleotides: Micelleplexes Outperform Polyplexes. *Biomacromolecules* **2022**, 23 (8), 3257–3271.
- (46) Tan, Z.; Jiang, Y.; Ganewatta, M. S.; Kumar, R.; Keith, A.; Twaroski, K.; Pengo, T.; Tolar, J.; Lodge, T. P.; Reineke, T. M. Block Polymer Micelles Enable CRISPR/Cas9 Ribonucleoprotein Delivery: Physicochemical Properties Affect Packaging Mechanisms and Gene Editing Efficiency. *Macromolecules* **2019**, 52 (21), 8197–8206.
- (47) Tan, Z.; Jiang, Y.; Zhang, W.; Karls, L.; Lodge, T. P.; Reineke, T. M. Polycation Architecture and Assembly Direct Successful Gene Delivery: Micelleplexes Outperform Polyplexes via Optimal DNA Packaging. *J. Am. Chem. Soc.* **2019**, *141* (40), 15804–15817.
- (48) Van Bruggen, C.; Hexum, J. K.; Tan, Z.; Dalal, R. J.; Reineke, T. M. Nonviral Gene Delivery with Cationic Glycopolymers. *Acc. Chem. Res.* **2019**, 52 (5), 1347–1358.
- (49) Hanson, M. G.; Grimme, C. J.; Santa Chalarca, C. F.; Reineke, T. M. Cationic Micelles Outperform Linear Polymers for Delivery of Antisense Oligonucleotides in Serum: An Exploration of Polymer Architecture, Cationic Moieties, and Cell Addition Order. *Bioconjug Chem.* **2022**, 33 (11), 2121–2131.
- (50) Souza, V.V.; Vitale, P.A.M.; Florenzano, F.H.; Salinas, R.K.; Cuccovia, I.M. A novel method for DNA delivery into bacteria using cationic copolymers. *Braz. J. Med. Biol. Res.* **2021**, *54* (5), No. e10743.
- (51) Munoz, K. A.; Hergenrother, P. J. Facilitating Compound Entry as a Means to Discover Antibiotics for Gram-Negative Bacteria. *Acc. Chem. Res.* **2021**, *54* (6), 1322–1333.
- (52) Wilke, K. E.; Francis, S.; Carlson, E. E. Activity-Based Probe for Histidine Kinase Signaling. J. Am. Chem. Soc. 2012, 134 (22), 9150–9153
- (53) Jiang, Y.; Lodge, T. P.; Reineke, T. M. Packaging pDNA by Polymeric ABC Micelles Simultaneously Achieves Colloidal Stability and Structural Control. *J. Am. Chem. Soc.* **2018**, *140* (35), 11101–11111.
- (54) Sprouse, D.; Jiang, Y.; Laaser, J. E.; Lodge, T. P.; Reineke, T. M. Tuning Cationic Block Copolymer Micelle Size by pH and Ionic Strength. *Biomacromolecules* **2016**, *17* (9), 2849–59.
- (55) Laaser, J. E.; Lohmann, E.; Jiang, Y.; Reineke, T. M.; Lodge, T. P. Architecture-Dependent Stabilization of Polyelectrolyte Complexes between Polyanions and Cationic Triblock Terpolymer Micelles. *Macromolecules* **2016**, 49 (17), 6644–6654.

- (56) Chase, O. M.; Espinasse, A.; Wilke, K. E.; Carlson, E. E. Exploration of the Effects of gamma-Phosphate-Modified ATP Analogues on Histidine Kinase Autophosphorylation. *Biochemistry* **2018**, *57* (29), 4368–4373.
- (57) Yang, H.; Xiao, X.; Zhao, X. S.; Hu, L.; Xue, X. F.; Ye, J. S. Study on Fluorescence Spectra of Thiamine and Riboflavin. *MATEC Web of Conferences* **2016**, *63*, 03013.
- (58) Galban, J.; Sanz-Vicente, I.; Navarro, J.; de Marcos, S. The intrinsic fluorescence of FAD and its application in analytical chemistry: a review. *Methods Appl. Fluoresc* **2016**, *4* (4), No. 042005.
- (59) Hughes, L. D.; Rawle, R. J.; Boxer, S. G. Choose Your Label Wisely: Water-Soluble Fluorophores Often Interact with Lipid Bilayers. *PLoS One* **2014**, *9* (2), No. e87649.
- (60) Zanetti-Domingues, L. C.; Tynan, C. J.; Rolfe, D. J.; Clarke, D. T.; Martin-Fernandez, M. Hydrophobic Fluorescent Probes Introduce Artifacts into Single Molecule Tracking Experiments Due to Non-Specific Binding. *PLoS One* **2013**, *8* (9), No. e74200.
- (61) Stiefel, P.; Schmidt-Emrich, S.; Maniura-Weber, K.; Ren, Q. Critical aspects of using bacterial cell viability assays with the fluorophores SYTO9 and propidium iodide. *BMC Microbiol* **2015**, *15*, 36.
- (62) Okoliegbe, I. N.; Hijazi, K.; Cooper, K.; Ironside, C.; Gould, I. M. Trends of Antimicrobial Resistance and Combination Susceptibility Testing of Multidrug-Resistant Pseudomonas aeruginosa Isolates from Cystic Fibrosis Patients: a 10-Year Update. *Antimicrob. Agents Chemother.* **2021**, *65* (6), e02483.
- (63) Ruseska, I.; Zimmer, A. Internalization mechanisms of cell-penetrating peptides. *Beilstein J. Nanotechnol* **2020**, *11*, 101–123.
- (64) Csepregi, R.; Lemli, B.; Kunsagi-Mate, S.; Szente, L.; Koszegi, T.; Nemeti, B.; Poor, M. Complex Formation of Resorufin and Resazurin with Beta-Cyclodextrins: Can Cyclodextrins Interfere with a Resazurin Cell Viability Assay? *Molecules* **2018**, 23 (2), 382.
- (65) Osaka, I.; Hefty, P. S. Simple resazurin-based microplate assay for measuring Chlamydia infections. *Antimicrob. Agents Chem.* **2013**, 57 (6), 2838–2840.
- (66) Albur, M.; Noel, A.; Bowker, K.; MacGowan, A. Bactericidal activity of multiple combinations of tigecycline and colistin against NDM-1-producing Enterobacteriaceae. *Antimicrob. Agents Chemother.* **2012**, *56* (6), 3441–3.
- (67) Cushnie, T. P.; O'Driscoll, N. H.; Lamb, A. J. Morphological and ultrastructural changes in bacterial cells as an indicator of antibacterial mechanism of action. *Cell. Mol. Life Sci.* **2016**, *73* (23), 4471–4492.
- (68) Kumar, R.; Santa Chalarca, C. F.; Bockman, M. R.; Bruggen, C. V.; Grimme, C. J.; Dalal, R. J.; Hanson, M. G.; Hexum, J. K.; Reineke, T. M. Polymeric Delivery of Therapeutic Nucleic Acids. *Chem. Rev.* **2021**, *121* (18), 11527–11652.
- (69) Kim, B. S.; Kim, H. J.; Osawa, S.; Hayashi, K.; Toh, K.; Naito, M.; Min, H. S.; Yi, Y.; Kwon, I. C.; Kataoka, K.; Miyata, K. Dually Stabilized Triblock Copolymer Micelles with Hydrophilic Shell and Hydrophobic Interlayer for Systemic Antisense Oligonucleotide Delivery to Solid Tumor. *ACS Biomater Sci. Eng.* **2019**, 5 (11), 5770–5780.
- (70) Rubinstein, E.; Keynan, Y. Vancomycin revisited 60 years later. Front Public Health 2014, 2, 217.
- (71) Glauert, A. M.; Thornley, M. J. The Topography of the Bacterial Cell Wall. *Annu. Rev. Microbiol.* **1969**, 23, 159–198.
- (72) Boix-Lemonche, G.; Lekka, M.; Skerlavaj, B. A Rapid Fluorescence-Based Microplate Assay to Investigate the Interaction of Membrane Active Antimicrobial Peptides with Whole Gram-Positive Bacteria. *Antibiotics (Basel)* **2020**, 9 (2), 92.
- (73) Lan, X. J.; Yan, H. T.; Lin, F.; Hou, S.; Li, C. C.; Wang, G. S.; Sun, W.; Xiao, J. H.; Li, S. Design, Synthesis and Biological Evaluation of 1-Phenyl-2-(phenylamino) Ethanone Derivatives as Novel MCR-1 Inhibitors. *Molecules* **2019**, *24* (15), 2719.
- (74) Hu, M.; Guo, J.; Cheng, Q.; Yang, Z.; Chan, E. W. C.; Chen, S.; Hao, Q. Crystal Structure of Escherichia coli originated MCR-1, a phosphoethanolamine transferase for Colistin Resistance. *Sci. Rep* **2016**, *6*, 38793.